NÖHÜ Müh. Bilim. Derg. / NOHU J. Eng. Sci., Erken Görünüm / InPress

Niğde Ömer Halisdemir Üniversitesi Mühendislik Bilimleri Dergisi
Niğde Ömer Halisdemir University Journal of Engineering Sciences

Araştırma makalesi / Research article

www.dergipark.org.tr/tr/pub/ngumuh / www.dergipark.org.tr/en/pub/ngumuh

Fabrication of CZTS thin film on flexible Cu-foil substrate by two-stage process

İki aşamalı yöntem ile CZTS ince filmlerinin esnek Cu-folyo altlık üzerine büyütülmesi

Mehmet Ali Olğar[1,*], Recep Zan[2]

[1,2] *Niğde Ömer Halisdemir University, Department of Physics, 51240, Niğde Türkiye*
[1,2] *Niğde Ömer Halisdemir University, Nanotechnology Application and Research Center, 51240, Niğde, Türkiye*

Abstract

In this research, CZTS thin films were grown on flexible Cu-foil substrates with varying sulfurization times. Distinct characterization methods were employed, including X-ray diffraction (XRD), Raman spectroscopy, Energy-Dispersive X-ray Spectroscopy (EDX), Scanning Electron Microscopy (SEM), optical transmission, and Photoluminescence (PL) measurements. Distinctive diffraction peaks characteristic of the kesterite CZTS phase were observed in the XRD analysis, occurring around at 2θ= 28.45° (112), 47° (220/204), and 56° (312/116). Additionally, some secondary phases such as Cu_2S and SnS were identified. Raman spectroscopy confirmed the presence of the kesterite CZTS phase, with a prominent peak detected at approximately ~336 cm^{-1}, attributed to sulfur atom vibrations within the kesterite structure. Apart from CZTS structure, minor peaks suggesting the presence of the Cu_2SnS_3 (CTS) phase was detected. EDX analysis revealed compositions with Cu-poor content and Zn-rich content across all samples, with slight variations in sulfurization dwell times affecting the chemical composition. SEM imaging at different magnifications showed alterations in surface morphology and grain structures. Films sulfurized for 30 s and 60 s displayed a granular structure morphology, while extending the dwell time to 120 s resulted in a more compact surface morphology. Optical band gap values ranged between 1.57 and 1.60 eV. PL measurements consistently exhibited strong PL emission around 1.25 eV for all samples, attributed to various transitions within the band structure of CZTS film. The absence of observable band-to-band transitions in the PL measurements indicated the presence of intrinsic defect levels and recombination centers within CZTS. Overall, it was demonstrated in this study that CZTS thin films can be produced on flexible Cu-foils with short sulfurization times, thereby expanding the application areas of CZTS thin-film solar cells.

Keywords: CZTS thin film, Cu-foil, Sputtering, RTP, Short sulfurization time

Öz

Bu araştırmada, farklı sülfürleme süreleri ile esnek Cu-folyo üzerine büyütülmüş CZTS ince filmler incelendi. X-ışını kırınımı (XRD), Raman spektroskopisi, Enerji Dağılımlı X-ışını spektroskopisi (EDX), Taramalı Elektron Mikroskopisi (SEM), optik geçirgenlik ve fotolüminesans (PL) ölçümleri de dahil olmak üzere çeşitli karakterizasyon yöntemleri kullanıldı. XRD analizinde kesterit CZTS fazına özgü belirgin kırınım pikleri 2θ= 28.45° (112), 47° (220/204) ve 56° (312/116) civarında meydana gelen pikler gözlemlendi. Ayrıca, Cu_2S ve SnS gibi bazı ikincil fazlar tespit edildi. Raman spektroskopisi, kesterit CZTS fazının varlığını doğruladı ve kesterit yapısı içindeki kükürt atomu titreşimlerine atfedilen yaklaşık ~336 cm^{-1}'de belirgin bir pik tespit edildi. CZTS yapısının yanı sıra, Cu_2SnS_3 (CTS) fazının varlığını işaret eden az sayıda pik de tespit edildi. EDX analizi, tüm örneklerin Cu-fakiri ve Zn-zengini kompozisyona sahip olduğunu göstermiştir. Farklı büyütme oranlarında yapılan SEM görüntülemeleri yüzey morfolojisinde ve tane yapılarında değişiklikler olduğunu gösterdi. 30 ve 60 saniye süreyle sülfürlenmiş filmler taneli bir yapı morfolojisi sergilerken, bekleme süresini 120 saniyeye uzatmak daha kompakt bir yüzey morfolojisine katkı sağladığı tespit edilmiştir. Optik bant aralığı değerleri 1.57 ile 1.60 eV arasında değişkenlik göstermiştir. PL ölçümleri, tüm örneklerde 1.25 eV civarında güçlü bir PL emisyonu sergiledi ve bu, CZTS yapısı içindeki çeşitli geçişlere atfedildi. PL ölçümlerinde gözlemlenen banttan banta geçişlerinin olmaması, CZTS içindeki özden kusur seviyeleri ve rekombinasyon merkezlerinin varlığını işaret ettiği belirlenmiştir. Genel olarak, bu çalışmada CZTS ince filmlerin kısa sülfürleme süreleriyle esnek Cu-folyolar üzerine üretilebileceği ve bu sayede CZTS ince film güneş pillerinin uygulama alanlarının genişletilebileceği gösterilmiştir.

Anahtar kelimeler: CZTS ince film, Cu-folyo, Saçtırma, RTP, Kısa sülfürleme süresi

1 Introduction

The CdTe and CIGS based thin film solar cells have already reached conversion efficiency above 20%, which is competitive with Si-based solar cells. However, toxicity of cadmium (Cd) and the limited availability of indium (In) and gallium (Ga) pose constraints on these thin film solar cells. In this context, Cu_2ZnSnS_4 (CZTS) thin film has emerged as

* Sorumlu yazar / Corresponding author, e-posta / e-mail: mehmetaliolgar@ohu.edu.tr (M. A. Olğar)
Geliş / Recieved: 01.04.2024 Kabul / Accepted: 02.05.2024 Yayımlanma / Published: xx.xx.20xx
doi: 10.28948/ngmuh.1462925

a highly promising absorber layer for photovoltaic industry (PV). It possesses several advantageous properties including the utilization of earth-abundant, environmental-friendly and cost-effective raw materials. Furthermore, CZTS exhibits a direct optical band gap of approximately 1.5 eV, which can be tuned to 1.0 eV by incorporation of Se into structure [1]. CZTS also demonstrates a high optical absorption coefficient (>10^4 cm^{-1}) in the visible range and exhibits p-type conductivity [2]. Moreover, CZTS boasts a theoretically high efficiency of approximately 30% according to the theoretical limit [3]. However, the current record conversion efficiency of CZTS stands at around 14% when fabricated on rigid glass substrates [4]. This indicates that there is considerable gap for improvement in enhancing the performance of CZTS as a thin film material for solar cells.

There exist various methods for the growth of CZTS thin films, categorized as physical (vacuum-based) and chemical (non-vacuum-based) growth methods. Physical methods include sputtering techniques such as DC and RF sputtering [5-7], thermal evaporation [8], pulsed laser deposition [9], e-beam evaporation [10], and etc. Chemical methods, on the other hand, encompass spin-coating [11], dip-coating [12], spray pyrolysis [13], electro-deposition [14], and similar approaches. Among these methods, sputtering is widely employed due to its ability to provide homogenous films with controlled thickness and the capability for large-scale production.

There are numerous strategies have been explored to optimize the structural, compositional, optical properties and also electrical characteristics of CZTS-based thin films to enhance conversion efficiency. These approaches involve the manipulation of various factors such as growth parameters (pressure, deposition rate, etc.) [15], chemical compositions (Cu-poor/Zn-rich or Cu-rich/Zn-rich) [16], annealing parameters (temperature, heating rate, dwell time, chalcogen source, etc.) [17], incorporation of different doping atoms (Al, In, Cd, Li, Ge, Ag, Na, K, etc.) [18-20], utilization of diverse back contact materials (Ag, Bi, Ti, Mo, etc.) [21], implementation of different interlayer materials (Al_2O_3, TiN, MoO_x, graphene, MoS_2, etc.) to achieve clear and well-defined interfaces [22, 23], utilization of a single quaternary target [24, 25] and exploration of different stacking orders [26] to enhance the homogeneity and crystal quality of the films. These strategies offer avenues for fine-tuning the features of the samples and advancing their performance in practical applications.

Thin film solar cells find application in various fields such as building integration, wearable technologies, space applications, and the automotive sector [27]. However, the use of rigid substrates limits their application in these fields, and therefore, flexible substrates are more preferred. The most common flexible substrates which used to growth CZTS thin film solar cells are stainless steel (SS) [28], aluminum (Al) [29], titanium (Ti) [30], molybdenum (Mo) [31], flexible glass (FG) [32], polyimide (P) [36], etc. Among these, FG and P substrates are organic-based and have a maximum sustainable temperature underlain by 500 °C, which is epically lower as compared with metal foils (Al, Ti, Mo, SS) that can withstand temperatures of 600 °C or higher [33].

Table 1 provides information on the price, electrical resistivity, and conductivity properties of various materials. Among the available metal foils, Mo foil is commonly used due to its linear thermal expansion coefficient of $5.2x10^{-6}$ K^{-1}. However, Mo foil is associated with drawbacks such as high price (76.67 USD/kg) [34], high resistivity (4.99×10^{-6} Ω.cm) [35], and low conductivity (17.9×10^6 S/m) [36] when compared to other materials. Therefore, there is a demand for a foil material that exhibits low cost, low resistivity, and high conductivity, enabling the fabrication of high-performance CZTS thin film solar cells. Among the listed materials, copper (Cu) foil possesses the most desirable properties, including lower cost (9.17 USD/kg) [34], lower resistivity (1.68×10^{-8} Ω.cm) [36], and higher electrical conductivity (5.96×10^7 S/m) [37]. Due to these advantageous properties, Cu foil is widely used as an electrical conductor in circuit boards, batteries, and solar energy appliances.

Work function of back contact, absorber layer, etc. is crucial for enhancing cell parameters and this can be important property to select the flexible foils for CZTS based thin film solar cells. If the work function of metal foil is smaller than semiconductor absorber layer, the Schottky contact is formed between the metal and semiconductor according to the Schottky contact model [38]. The work function of CZTS absorber layer is ~5.7 eV [39] and work function of Cu, Mo, Ti and Al foil which presented in Table 1 is determined as 5.10 eV, 5.0 eV, 4.33 eV, and 4.2 eV, respectively. The enhanced work function is belong to the Cu foil and the higher work function of back contact (foil) is enhance to the built-in potential of device [40]. The built-in potential is a consequence of the potential decrease across the width of the absorber layer. This gradual decrease in potential is responsible for generating an electric field directed towards the p-n junction. Consequently, this electric field drives the charge carriers towards the junction. Moreover, the electric field induces an increase in the diffusion length of carriers, enhancing their collection on the n-side of the junction. In the literature, the open-circuit voltage (V_{OC}) exhibits high sensitivity to changes in Φ_M values, while the short-circuit current (J_{SC}) and fill factor (FF) demonstrate relatively minor dependence on Φ_M [38].

Table 1. Properties of some metals

Subs.	Price (USD/kg) [34, 41]	Resistivity (Ω.cm) [35, 42]	Conductivity (S/m) [36, 43]	Work Function (eV) [44, 45]	Therm. Exp. (K^{-1}) at >500 K° [40, 46, 47]
Cu	9.17	1.68×10^{-8}	5.96×10^7	5.10	$16x10^{-6}$
Mo	76.67	4.99×10^{-6}	17.9×10^6	5.0	$4.8x10^{-6}$
Ti	8.26	4.20×10^{-7}	2.38×10^6	4.33	$8.4\text{-}8.6x10^{-6}$
Al	2.56	2.82×10^{-8}	3.5×10^7	4.2	$21x10^{-6}$

In light of all this information, in this study, CZTS thin films will be produced for the first time on Cu foil using Cu-foil/ZnS/Cu/Sn/Cu stacking order (and RTP method. To investigate the impact of different sulfurization times on the properties of the CZTS thin films, we tested short dwell times (30, 60 and 120 sec.) at reaction temperature of 425 °C. By varying the dwell times, we aimed to understand how it affected the structural, optical, and electrical properties of the CZTS thin films. It should be noted that higher reaction temperatures (> 425°C) have been tried for fabrication of CZTS thin films. However, the most suitable temperature has been determined to be 425°C due to occurrences of fragmentation and detachment on the substrate surface.

2 Material and methods

2.1 Cleaning of substrates

The study involved a specific pre-treatment process for the glass and flexible Cu-foil substrates before the CZTS thin film deposition. The pre-treatment steps are as follows:

a) The glass substrate was cleaned for 5 minutes in an ultrasonic bath with acetone.
b) Then, it was cleaned for another 5 minutes in an ultrasonic bath with isopropanol alcohol (IPA).
c) Finally, it was cleaned for 10 minutes in an ultrasonic bath with distilled water (DW).
d) After the cleaning process, all substrates (both glass and flexible Cu-foils) were dried using N_2 gas.
e) All substrates, after the drying process, were exposed to an ultrasonic plasma cleaner system for 30 minutes. The ultrasonic plasma cleaning is a method used to remove any remaining impurities and contaminants from the substrate surfaces, ensuring a clean surface for thin film deposition.
f) Once the plasma cleaning was completed, the substrates were placed in a PVD system. Before starting the deposition process, a bias voltage was applied to the substrates for 10 min. This step was carried out under a vacuum level of < $2x10^{-6}$ Torr, ensuring a low-pressure environment to prevent contamination during the deposition process.

The purpose of these pre-treatment steps is to create a clean and well-prepared surface for the subsequent CZTS thin film deposition. Proper cleaning and surface preparation are crucial in ensuring good adhesion and quality of the deposited CZTS thin films, which, in turn, will impact the performance of the fabricated CZTS thin film solar cells.

2.2 Deposition of CZTS precursor and thin films

The CZTS samples were grown on glass and flexible Cu-foils using sputtering and RTP methods, respectively. Firstly, high purity Cu (5N), Sn (5N) and ZnS (4N) sputter targets were used to form stacks on flexible Cu-foils via magnetron sputtering (DC and RF). Cu layers were deposited using a DC power supply, while the Sn and ZnS layers were deposited using an RF power supply. Deposition parameters such as $2x10^{-6}$ mTorr base pressure, 10^{-3} mTorr operating pressure, 0.9-1.0 Å/s deposition rate was used for the deposition of Cu, Sn and ZnS precursor films. The thickness of ZnS, Cu, Sn, and Cu layers was given in our previously study [48]. The second stage of fabrication is annealing of precursor layers to form CZTS thin films by RTP system. Annealing parameters of Cu foil/CZTS were illustrated in Table 2. Cu-foil/CZTS samples were labeled as CZTS-30, CZTS-60, and CZTS-120.

Table 2. The sample ID, stacking order and annealing parameters of CZTS precursor films

Sample ID	Stacking Order	Annealing Parameters
CZTS-30	Cu-foil/ZnS/Cu/Sn/Cu	425 °C, 1 °C/s, 30 s, 5 mg S
CZTS-60		425 °C, 1 °C/s, 60 s, 5 mg S
CZTS-120		425 °C, 1 °C/s, 120 s, 5 mg S

2.3 Characterization of CZTS thin films

The chemical composition and structural properties of all samples were determined using various techniques. Energy-dispersive X-ray (EDX) spectroscopy, X-ray diffractometry (XRD) (PANalytical-EMPYREAN instrument), and Raman spectroscopy (Renishaw inVia Spectrometer) were employed for structural characterization. EDX measurements were performed on a 115×135 μm^2 area, and XRD patterns were obtained using CuKα (λ = 1,5406 Å) radiation. Raman spectroscopy measurements performed by 633 nm of wavelength. Additionally, scanning electron microscopy (SEM) using a ZEISS-GeminiSEM instrument was utilized to examine the surface properties of the samples.

The optical properties of the samples were determined using two techniques: spectroscopic ellipsometry (J.A. Woollam Co., Inc.) and photoluminescence (PL). Transmittance measurements were conducted on samples deposited on glass substrates ranging from 620 nm to 1240 nm. Room temperature PL measurements were obtained using a hybrid Raman spectroscopy system employing laser excitation wavelength of 633 nm.

3 Result and discussion

The EDX analysis of precursor films annealed using 30 s, 60 s, and 120 s dwell times deposited on flexible Cu-foil at 425 °C reaction temperature to form CZTS films are given in Table 3. In Table 3, regardless of dwell times, all samples exhibited Cu-poor (Cu/(Zn+Sn)<1) chemical compositions. However, it was observed that, only sample which annealed using 30 dwell time had Zn-rich (Zn/Sn>1) composition, while samples which annealed by using 60 and 120 s dwell times had stoichiometric Zn (Zn/Sn=1) composition. The Cu-poor and Zn-rich chemical composition is a desired property for CZTS-based thin film solar cells, as this composition gives rise to the formation of Cu vacancies (V_{Cu}) and Cu_{Zn} antisite defects. These defects contribute to achieving strong p-type conductivity and, consequently, higher solar cell performance [48].

The diffraction pattern of annealed samples for 30 s, 60 s, and 120 s dwell times on flexible Cu-foil was presented in Figure 1. The main diffraction peaks of CZTS samples observed at around 2θ = ~28.45° (112), ~47° (220/204) and ~56° (312/116) that are attributed to kesterite CZTS structure (98-018-4358). The other observed peaks are also marked on the Figure 1. Also, the diffraction peaks at 2θ = ~43.25°, and

~50.40° positions stemming from the Cu-foil (98-062-7117) were observed. Moreover, the peak we determined at 2θ = ~38.9° position was attributed to the SnS secondary phase (98-006-7442) and peaks at around 2θ = 27.20°, 39.8°, 40.75°, 45.75°, 48.41°, 53.71° and 54.96° are attributed to the Cu_2S secondary phase (98-002-3596). It is predicted that the formation of the Cu_2S phase which detected in the diffraction patterns is caused by the interaction of the sulfur vapor with the Cu foil. In addition, the formation of SnS phase which observed in XRD patterns is due to the inability to provide sufficient sulfur vapor pressure in the structure due to low reaction temperature. It was determined that the diffraction peaks of the mentioned secondary phases decreased significantly by increasing the dwell time from 30 to 120 s [49].

Table 3. The EDX measurements of the sulfurized samples on flexible Cu-foil using different dwell times

Sample	Atomic Weight (%)				Atomic Ratio		
	Cu	Zn	Sn	S	Cu/ (Zn+Sn)	Zn/ Sn	S/ Metal
CZTS-30	22.4	12.4	12.0	53.2	0.92	1.03	1.13
CZTS-60	22.1	12.3	12.2	53.4	0.90	1.00	1.15
CZTS-120	21.9	12.1	12.1	53.8	0.91	1.00	1.17

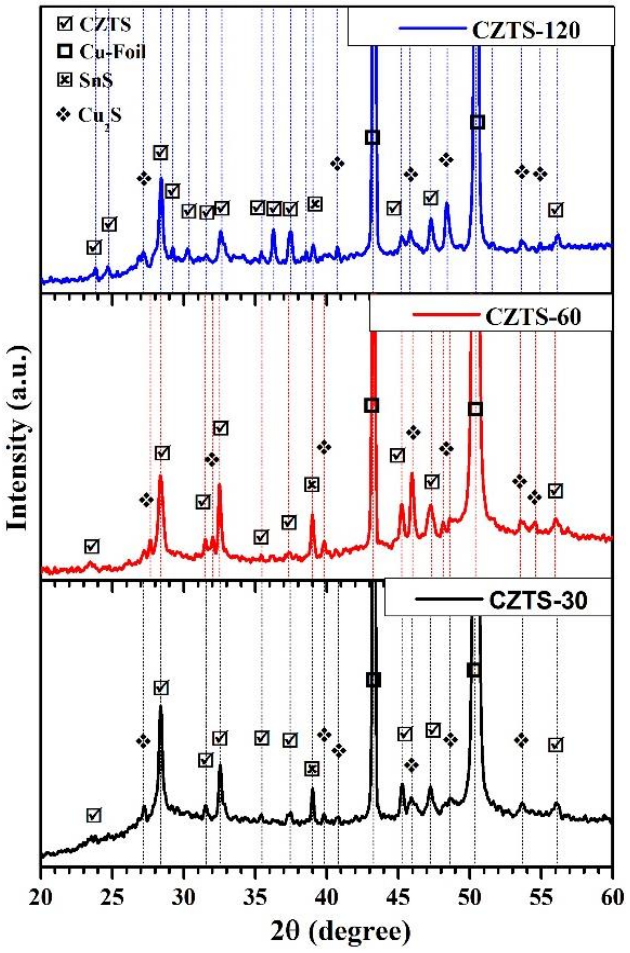

Figure 1. The XRD pattern of annealed samples for 30 s, 60 s and 120 s sulfurization times

In order to investigate and compare crystal quality of the samples, some structural parameters of CZTS thin films were determined by using main diffraction peak belongs to (112) diffraction plane of kesterite CZTS structure. First, the Debye-Scherrer formula (Equation (1)) were used to calculate the crystallite size (D) of films by using the Full Width Half Maximum (FWHM) values (β) of the (112) diffraction peak. In addition, the micro-strain values (ε) inside the lattice were calculated by Equation (2). The dislocation density (δ) and the number of crystals per unit surface area (N) were determined with Equation (3) and Equation (4). *T* represents thickness of the film. Moreover, the inter-planar spacing and lattice parameters such as a and c were calculated by using Equation (5) and Equation (6).

$$D = \frac{K.\lambda}{\beta.\cos\theta} \quad (1)$$

$$\varepsilon = \frac{\beta.\cos\theta}{4} \quad (2)$$

$$\delta = \frac{1}{D^2} \quad (3)$$

$$N = \frac{T}{D^3} \quad (4)$$

$$d = \frac{\lambda}{2*\sin(\theta)} \quad (5)$$

$$\frac{1}{d^2} = \frac{h^2+k^2}{a^2} + \frac{l^2}{c^2} \quad (6)$$

The crystallite sizes of kesterite CZTS films sulfurized for 30, 60, and 120 s dwell times were found to be 34.51 nm, 22.88 nm, and 32.18 nm, respectively. In addition, for 30 s, 60 s and 120 s sulfurization dwell times, $1.05x10^{-3}$, $1.58x10^{-3}$, $1.13x10^{-3}$ micro-strain, $8.4x10^{-4}$, $1.9x10^{-3}$, $9.6x10^{-4}$ dislocation density, $3.4x10^{-2}$, $11.6x10^{-2}$, $4.2x10^{-2}$ number of crystal per unit surface area values were calculated and presented in Table 4. As a result of the calculations, it was seen that CZTS-30 thin film exhibited higher crystallite size and better structural properties. The smaller crystallite size means that formation of more grain boundaries and accordingly more recombination centers for charge carriers [50]. Furthermore, in the lattice, increasing or decreasing of the strain can change all the physical properties of the films (for example, the position of the atoms). Additionally, secondary phase formations (Cu_2S, SnS, etc.) causes to decrease the active region in the films, the shunt resistance and accordingly cell performance [51].

The diffraction patterns of kesterite CZTS phase is similar with some other secondary phases (CTS, ZnS, etc.) [52]. Thus, Raman spectra was used as a complementary technique. The Raman spectra of annealed films for different sulfurization times (30, 60, and 120 s) are given in Figure 2. Considering the Figure 2, irrespective of the sulfurization times, the main peak position was observed at around ~336-338 cm^{-1} which is attributed to the kesterite phase in all samples. This peak is ascribed to vibration of S atoms in kesterite structure [53, 54]. The other peaks are marked on the graphs [55, 56]. Apart from Raman modes of kesterite

phase, the minor peaks determined in all samples at around 292-298 cm^{-1} are associated with the Cu_2SnS_3 (CTS) phase [57, 58].

Table 4. The structural parameters of CZTS samples sulfurized for 30 s, 60 s and 120 s dwell times

Parameters	CZTS-30	CZTS-60	CZTS-120
2θ (°)	28.39	28.40	28.41
FWHM (°)	0.248	0.374	0.266
D (nm)	34.51	22.88	32.18
ε (a.u.)	$1.05x10^{-3}$	$1.58x10^{-3}$	$1.13x10^{-3}$
δ (nm^{-2})	$8.4x10^{-4}$	$1.9x10^{-3}$	$9.6x10^{-4}$
N (nm^{-2})	$3.4x10^{-2}$	$11.6x10^{-2}$	$4.2x10^{-2}$
d (Å)	3.1412	3.1401	3.1339
a (Å)	5.4356	5.4269	5.4356
c (Å)	10.9023	10.9261	10.8797
c/2a	1.0028	1.0067	1.0008

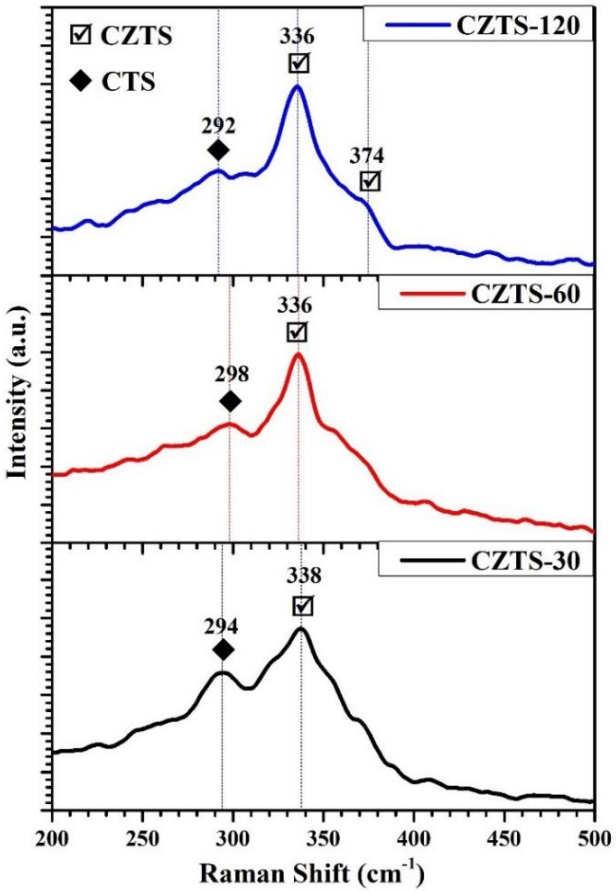

Figure 2. The Raman spectra of annealed samples with different sulfurization dwell times

The effect of sulfurization time on the surface morphologies and microstructure features of all samples were determined by SEM measurements employing two different magnifications (10 kX and 50 kX). The SEM images of CZTS thin films grown on the flexible Cu-foil using different sulfurization times are given in Figure 3. It was observed that all samples had dense and homogenous polycrystalline surface structure. CZTS samples which are sulfurized for 30 and 60 s dwell times have a granular structure morphology (Figure 3a-d). After sulfurization time increased from 60 to 120 s (Figure 3e, f), the grain boundaries were disappeared, and the more compact surface morphology was formed.

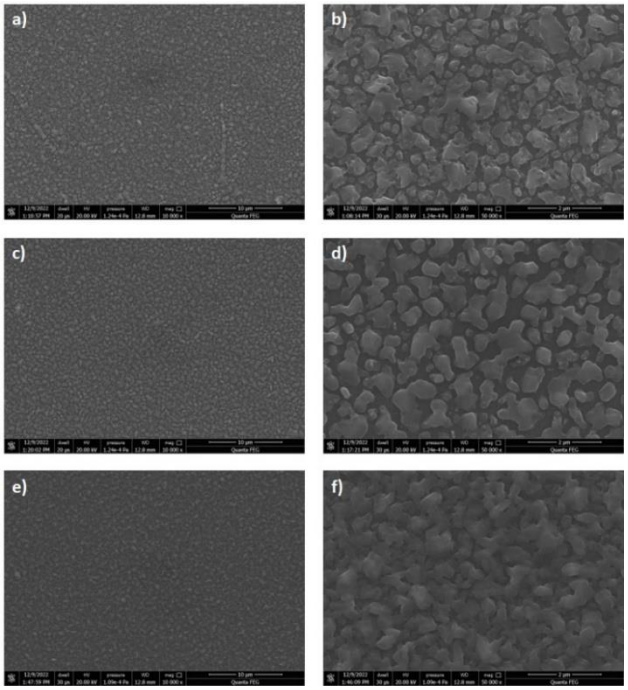

Figure 3. The SEM images of kesterite samples sulfurized for different dwell times; (a-b) 30 s, (c-d) 60 s, (e-f) 120 s

Optical properties of CZTS thin films grown on Cu foil using various sulfurization times (30 s, 60 s, and 120 s) characterized by two distinct approaches. In the first method, CZTS thin films were deposited on glass substrates to ascertain the optical band gaps by employing optimized sulfurization parameters for Cu-foil based samples. The optical band gap of the CZTS thin films was calculated based on the absorption coefficient (α), as determined by applying the Lambert-Beer law outlined in Equation (7) [59]:

$$\alpha = \frac{1}{d}\ln\left(\frac{1}{T}\right) \quad (7)$$

where, T and d are transmission and thickness parameters of the film. After calculating α, absorption coefficient spectra were given in Figure 4a. It was observed that all samples have absorption coefficient above 10^4 cm^{-1}. However, CZTS-30 thin film has slightly higher than the others. In addition, the Tauc plot [60] was used to estimate the optical band gap of the films using Equation (8);

$$(\alpha h\upsilon)^2 = A(h\upsilon - E_g) \quad (8)$$

where, A represents a constant, hυ denotes photon energy, and E_g signifies the optical band gap energy of the films. The optical band gap was ascertained through the plot of $(\alpha h\upsilon)^2$ against photon energy (eV), as depicted in Figure 4b. Figure 4b displays the determination of the optical band gap for CZTS thin films, yielding values of 1.57 eV, 1.58 eV, and 1.60 eV for sulfurization times of 30 s, 60 s, and 120 s,

respectively. Notably, these obtained optical band gap values align with previously reported findings in the literature [61]. The minor variations observed in the optical band gaps (ranging from 1.57 eV to 1.60 eV) have been attributed to the presence of secondary phases within the kesterite structure. Consequently, these slight differences in the chemical composition of the films and the stresses induced within the structure by these secondary phases are believed to be contributing factors [62].

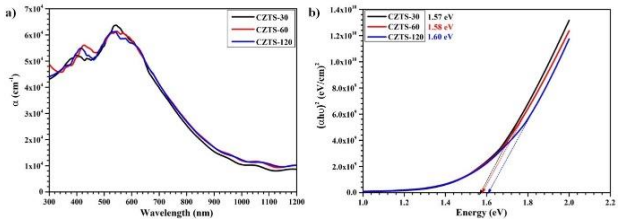

Figure 4. The plots for absorption coefficient and optical band gap of CZTS samples

The optical properties of CZTS thin films subjected to various sulfurization dwell times were additionally assessed through room temperature PL measurements, as illustrated in Figure 5. In all cases, the films displayed a prominent PL emission at approximately 1.25 eV. When comparing the band gap values and PL emissions of these samples (as depicted in Figure 4), it is reasonable to suggest that the PL emissions can be ascribed to transitions occurring from the conduction band to acceptor energy levels, band tailing, or other defect levels (such as V_{Cu}, Cu_{Zn}, etc.) [63]. In summary, the lack of observable band-to-band transitions in the PL measurements can be linked to the intrinsic defect levels and recombination centers present within the CZTS structure [64].

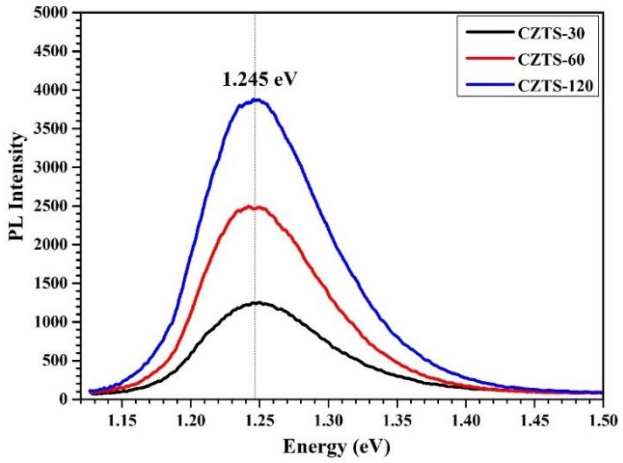

Figure 5. Room temperature PL measurements of CZTS thin films sulphurized with different dwell times

4 Conclusion

This study presents a detailed investigation of kesterite CZTS thin films deposited on flexible Cu-foil with varying sulfurization dwell times. The XRD analysis identified distinctive kesterite CZTS phase peaks at 2θ= 28.45° (112), 47° (220/204), and 56° (312/116). Additional peaks corresponding to Cu-foil, Cu_2S secondary phase, and SnS secondary phase were also observed. Raman spectroscopy confirmed the kesterite phase, notably with a dominant peak at ~336 cm^{-1} attributed to S atom vibrations within the kesterite structure. Minor peaks indicated the presence of Cu_2SnS_3 (CTS) phase not discernible by XRD. EDX analysis revealed consistent Cu-poor and Zn-rich compositions across for some samples, with slight variations due to sulfurization dwell times. SEM imaging at different magnifications (10 kX and 50 kX) displayed changes in surface morphology and grain structures. Films sulfurized for 30 s and 60 s exhibited a granular structure, whereas extending to 120 s resulted in a more compact surface. Optical band gap values ranged from 1.57 to 1.60 eV. PL measurements consistently showed strong emission at around 1.25 eV for all samples, indicating transitions related to defect levels within the CZTS structure. The absence of observable band-to-band transitions in PL suggested the presence of intrinsic defect levels and recombination centers within CZTS. These findings provide significant insights into developing sustainable and efficient solar energy utilizing flexible Cu-foil as a promising substrate for CZTS-based thin film solar cells.

Acknowledgment

The authors gratefully acknowledge the funding from The Scientific and Technological Research Council of Turkey (TÜBİTAK-120F275). The authors also acknowledge Serkan Erkan for his experimental support during this study.

Conflict of interest

The authors declare that there is no conflict of interest.

Similarity rate (iThenticate): 17 %

References

[1] A. Luque and S. Hegedus, Handbook of photovoltaic science and engineering, John Wiley & Sons, 2011.

[2] H. Katagiri, N. Ishigaki, T. Ishida and K. Saito, Characterization of Cu2ZnSnS4 thin films prepared by vapor phase sulfurization, Japanese Journal of Applied Physics, 40, 500, 2001. https://doi.org/10.1143/JJAP.40.500.

[3] W. Shockley and H.J. Queisser, Detailed balance limit of efficiency of p-n junction solar cells, 32, 510-519, 1961.

[4] Y. Gong, Q. Zhu, B. Li, S. Wang, B. Duan, L. Lou, C. Xiang, E. Jedlicka, R. Giridharagopal and Y. Zhou, Elemental de-mixing-induced epitaxial kesterite/CdS interface enabling 13%-efficiency kesterite solar cells, Nature Energy, 1-12, 2022. https://doi.org/10.1038/s41560-022-01132-4

[5] J. Jiang, L. Zhang, W. Wang and R. Hong, The role of sulphur in the sulfurization of CZTS layer prepared by DC magnetron sputtering from a single quaternary ceramic target, Ceramics International, 44, 11597-11602, 2018. https://doi.org/10.1016/j.ceramint.2018.03.225

[6] N. Akcay, E. Zaretskaya and S. Ozcelik, Development of a CZTS solar cell with CdS buffer layer deposited by RF magnetron sputtering, Journal of Alloys and Compounds, 772, 782-792, 2019. https://doi.org/10.1016/j.jallcom.2018.09.126.

[7] M.A. Olgar, A. Seyhan, A.O. Sarp and R. Zan, The choice of Zn or ZnS layer in the stacked precursors for preparation of Cu2ZnSnS4 (CZTS) thin films, Superlattice Microst, 146, 106669, 2020. https://doi.org/10.1016/j.spmi.2020.106669.

[8] E. Garcia-Llamas, J. Merino, R. Gunder, K. Neldner, D. Greiner, A. Steigert, S. Giraldo, V. Izquierdo-Roca, E. Saucedo and M. León, Cu2ZnSnS4 thin film solar cells grown by fast thermal evaporation and thermal treatment, Solar Energy, 141, 236-241, 2017. https://doi.org/10.1016/j.solener.2016.11.035.

[9] A. Lokhande, R. Chalapathy, J. Jang, P. Babar, M. Gang, C. Lokhande and J.H. Kim, Fabrication of pulsed laser deposited Ge doped CZTSSe thin film based solar cells: Influence of selenization treatment, Solar Energy Materials and Solar Cells, 161, 355-367, 2017. https://doi.org/10.1016/j.solmat.2016.12.016.

[10] M. Azim-Araghi and N. Safaie, Structural, optical and electrical properties of Cu2ZnSnS4 thin film deposited by electron beam evaporation method, Optik, 258, 168936, 2022. https://doi.org/10.1016/j.ijleo.2022.168936.

[11] H. Xin, J.K. Katahara, I.L. Braly and H.W. Hillhouse, 8% Efficient Cu2ZnSn(S,Se)4 solar cells from redox equilibrated simple precursors in DMSO, Advanced Energy Materials, 4, 1301823, 2014. https://doi.org/10.1002/aenm.201301823.

[12] A. Ziti, B. Hartiti, H. Labrim, S. Fadili, H.J. Tchognia Nkuissi, A. Ridah, M. Tahri and P. Thevenin, Effect of copper concentration on physical properties of CZTS thin films deposited by dip-coating technique, Applied Physics A, 125, 1-9, 2019. https://doi.org/10.1007/s00339-019-2513-0.

[13] M. Courel, E. Valencia-Resendiz, J. Andrade-Arvizu, E. Saucedo and O. Vigil-Galán, Towards understanding poor performances in spray-deposited Cu2ZnSnS4 thin film solar cells, Solar energy materials and solar cells, 159, 151-158, 2017. https://doi.org/10.1016/j.solmat.2016.09.004.

[14] C. Chan, H. Lam and C. Surya, Preparation of Cu2ZnSnS4 films by electrodeposition using ionic liquids, Solar Energy Materials and Solar Cells, 94, 207-211, 2010. https://doi.org/10.1016/j.solmat.2009.09.003.

[15] S. Alamri, Effect of Working Pressure on the Composition of a Cu2ZnSnS4 Thin Film Deposited by RF Sputtering of a Single Target, Arabian Journal for Science and Engineering, 1-8, 2022. https://doi.org/10.1007/s13369-022-06991-3.

[16] A. Moholkar, S. Shinde, G.L. Agawane, S. Jo, K. Rajpure, P. Patil, C. Bhosale and J. Kim, Studies of compositional dependent CZTS thin film solar cells by pulsed laser deposition technique: An attempt to improve the efficiency, Journal of Alloys and Compounds, 544, 145-151, 2012. https://doi.org/10.1016/j.jallcom.2012.07.108.

[17] M.A. Olgar, S. Erkan and R. Zan, Dependence of CZTS thin film properties and photovoltaic performance on heating rate and sulfurization time, J Alloy Compd, 963, 171283, 2023. https://doi.org/10.1016/j.jallcom.2023.171283.

[18] O.P. Singh, A. Sharma, K. Gour, S. Husale and V. Singh, Fast switching response of Na-doped CZTS photodetector from visible to NIR range, Solar Energy Materials and Solar Cells, 157, 28-34, 2016. https://doi.org/10.1016/j.solmat.2016.04.058.

[19] A. Migdadi, F.Y. Alzoubi, H. Al-Khateeb and M. Alqadi, Structural and optoelectronic characterization of synthesized undoped CZTS and Cd-doped CZTS thin films, 60, 138-149, 2022. https://doi.org/10.56042/ijpap.v60i2.54638.

[20] K. Kaur, K. Arora, B. Behzad, Q. Qiao and M. Kumar, Nanoscale charge transport and local surface potential distribution to probe defect passivation in Ag doped Cu2ZnSnS4 absorbing layer, Nanotechnology, 30, 065706, 2018. https://doi.org/10.1088/1361-6528/aaf185.

[21] S. Englund, Alternative back contacts for CZTS thin film solar cells, in, Acta Universitatis Upsaliensis, 2020.

[22] E. Ojeda-Durán, K. Monfil-Leyva, J. Andrade-Arvizu, I. Becerril-Romero, Y. Sánchez, R. Fonoll-Rubio, M. Guc, Z. Jehl, J. Luna-López and A. Muñoz-Zurita, CZTS solar cells and the possibility of increasing VOC using evaporated Al2O3 at the CZTS/CdS interface, Solar Energy, 198, 696-703, 2020. https://doi.org/10.1016/j.solener.2020.02.009.

[23] M. Vishwakarma, N. Thota, O. Karakulina, J. Hadermann and B. Mehta, Role of graphene inter layer on the formation of the MoS2-CZTS interface during growth, in: AIP Conf. Proc., AIP Publishing LLC, 1953 100064, 2018. https://doi.org/10.1063/1.5033000.

[24] J. He, L. Sun, K. Zhang, W. Wang, J. Jiang, Y. Chen, P. Yang and J. Chu, Effect of post-sulfurization on the composition, structure and optical properties of Cu2ZnSnS4 thin films deposited by sputtering from a single quaternary target, Applied Surface Science, 264, 133-138, 2013. https://doi.org/10.1016/j.apsusc.2012.09.140.

[25] M.A. Olgar, A. Seyhan, A.O. Sarp and R. Zan, Impact of sulfurization parameters on properties of CZTS thin films grown using quaternary target, J Mater Sci-Mater El, 31, 20620-20631, 2020. https://doi.org/10.1007/s10854-020-04582-2.

[26] M.A. Olgar, Enhancement in photovoltaic performance of CZTS Thin-film solar cells through varying stacking order and sulfurization time, J Mater Sci-Mater El, 33, 20121-20133, 2022. https://doi.org/10.1007/s10854-022-08829-y.

[27] J. Ajayan, D. Nirmal, P. Mohankumar, M. Saravanan, M. Jagadesh and L. Arivazhagan, A review of photovoltaic performance of organic/inorganic solar

cells for future renewable and sustainable energy technologies, Superlattices and Microstructures, 143, 106549, 2020. https://doi.org/10.1016/j.spmi.2020.106549.

[28] K. Ahn, S.-Y. Kim, S. Kim, D.-H. Son, S.-H. Kim, S. Kim, J. Kim, S.-J. Sung, D.-H. Kim and J.-K. Kang, Flexible high-efficiency CZTSSe solar cells on stainless steel substrates, Journal of Materials Chemistry A, 7, 24891-24899, 2019. https://doi.org/10.1039/C9TA08265D.

[29] Q. Tian, X. Xu, L. Han, M. Tang, R. Zou, Z. Chen, M. Yu, J. Yang and J. Hu, Hydrophilic Cu 2 ZnSnS 4 nanocrystals for printing flexible, low-cost and environmentally friendly solar cells, CrystEngComm, 14, 3847-3850, 2012. https://doi.org/10.1039/C2CE06552E.

[30] L. Sun, H. Shen, H. Huang, A. Raza, Q. Zhao and J. Yang, Influence of Ge layer location on performance of flexible CZTSSe thin film solar cell, Vacuum, 165, 186-192, 2019. https://doi.org/10.1016/j.vacuum.2019.04.026.

[31] Y. Zhang, Q. Ye, J. Liu, H. Chen, X. He, C. Liao, J. Han, H. Wang, J. Mei and W. Lau, Earth-abundant and low-cost CZTS solar cell on flexible molybdenum foil, Rsc Advances, 4, 23666-23669, 2014. https://doi.org/10.1039/C4RA02064B.

[32] C.-Y. Peng, T.P. Dhakal, S. Garner, P. Cimo, S. Lu and C.R. Westgate, Fabrication of Cu2ZnSnS4 solar cell on a flexible glass substrate, Thin Solid Films, 562, 574-577, 2014. https://doi.org/10.1016/j.tsf.2014.03.054.

[33] I. Becerril-Romero, L. Acebo, F. Oliva, V. Izquierdo-Roca, S. López-Marino, M. Espíndola-Rodríguez, M. Neuschitzer, Y. Sánchez, M. Placidi and A. Pérez-Rodríguez, CZTSe solar cells developed on polymer substrates: Effects of low-temperature processing, Progress in Photovoltaics: Research and Applications, 26, 55-68, 2018. https://doi.org/10.1002/pip.2945.

[34] M. Insider, Price of Metals, 2023.

[35] M. Ohring, Engineering materials science, Elsevier, 1995.

[36] P. Desai, T. Chu, H.M. James and C. Ho, Electrical resistivity of selected elements, Journal of physical and chemical reference data, 13, 1069-1096, 1984. https://doi.org/10.1063/1.555723.

[37] ThoughtCo., Table of Electrical Resistivity and Conductivity, 2023.

[38] S. Zee, Physics of semiconductor devices/In 2 books. Book. 1. Per. from English.-2nd revision. and additional ed, M.: Mir, 1984.

[39] A. Kumar and A.D. Thakur, Role of contact work function, back surface field, and conduction band offset in Cu2ZnSnS4 solar cell, Japanese Journal of Applied Physics, 57, 08RC05, 2018. https://doi.org/10.7567/JJAP.57.08RC05.

[40] T. Jäger, Y.E. Romanyuk, B. Bissig, F. Pianezzi, S. Nishiwaki, P. Reinhard, J. Steinhauser, J. Schwenk and A.N. Tiwari, Improved open-circuit voltage in Cu (In, Ga) Se2 solar cells with high work function transparent electrodes, Journal of Applied Physics, 117, 2015. https://doi.org/10.1063/1.4922351.

[41] B. Theler, S.K. Kauwe and T.D. Sparks, Materials Abundance, Price, and Availability Data from the Years 1998 to 2015, Integrating Materials and Manufacturing Innovation, 9, 144-150, 2020. https://doi.org/10.1007/s40192-020-00173-5.

[42] U. Ugur and G. Elert, Resistivity of steel, in: The physics factbook, School Sci., 2006.

[43] L. MatWeb, Material property data, MatWeb,[Online]. Available: http://www. matweb. com, 2016.

[44] J. Hölzl and F.K. Schulte, Work function of metals, Solid surface physics, 1-150, 2006.

[45] B. Singh and B. Mehta, Relationship between nature of metal-oxide contacts and resistive switching properties of copper oxide thin film based devices, Thin Solid Films, 569, 35-43, 2014. https://doi.org/10.1016/j.tsf.2014.08.030

[46] Best Research-Cell Efficiency chart, regularly updated by NREL, http://www.nrel.gov/ncpv/images/efficiency_chart.jpg , 2021.

[47] E. ToolBox, Thermal Expansion - Linear Expansion Coefficients, 2023.

[48] S. Chen, A. Walsh, X.G. Gong and S.H. Wei, Classification of lattice defects in the kesterite Cu2ZnSnS4 and Cu2ZnSnSe4 earth-abundant solar cell absorbers, Adv Mater, 25, 1522-1539, 2013. https://doi.org/10.1002/adma.201203146

[49] H.R. Jung, S.W. Shin, K. Gurav, M. Suryawanshi, C.W. Hong, H.S. Yang, J.Y. Lee, J.H. Moon and J.H. Kim, Phase evolution of Cu2ZnSnS4 (CZTS) kesterite thin films during the sulfurization process, Ceramics International, 41, 13006-13011, 2015. https://doi.org/10.1016/j.ceramint.2015.06.145.

[50] Y. Wei, D. Zhuang, M. Zhao, Q. Gong, R. Sun, G. Ren, Y. Wu, L. Zhang, X. Lyu and X. Peng, An investigation on the relationship between open circuit voltage and grain size for CZTSSe thin film solar cells fabricated by selenization of sputtered precursors, Journal of alloys and compounds, 773, 689-697, 2019. https://doi.org/10.1016/j.jallcom.2018.09.258.

[51] B.G. Mendis, M.C. Goodman, J.D. Major, A.A. Taylor, K. Durose and D.P. Halliday, The role of secondary phase precipitation on grain boundary electrical activity in Cu2ZnSnS4 (CZTS) photovoltaic absorber layer material, Journal of applied physics, 112, 124508, 2012. https://doi.org/10.1063/1.4769738

[52] M.A. Olgar, B.M. Basol, M. Tomakin and E. Bacaksiz, Phase transformation in Cu2SnS3 (CTS) thin films through pre-treatment in sulfur atmosphere, J Mater Sci-Mater El, 32, 10018-10027, 2021. https://doi.org/10.1007/s10854-021-05660-9

[53] P. Fernandes, P. Salomé and A. Da Cunha, Study of polycrystalline Cu2ZnSnS4 films by Raman scattering, Journal of alloys and compounds, 509, 7600-7606, 2011. https://doi.org/10.1016/j.jallcom.2011.04.097

[54] M. Guc, S. Levcenko, I.V. Bodnar, V. Izquierdo-Roca, X. Fontane, L.V. Volkova, E. Arushanov and A. Pérez-

Rodríguez, Polarized Raman scattering study of kesterite type Cu2ZnSnS4 single crystals, Scientific reports, 6, 1-7, 2016. https://doi.org/10.1038/srep19414

[55] P. Prabeesh, V. Sajeesh, I.P. Selvam, M.D. Bharati, G.M. Rao and S.J.S.E. Potty, CZTS solar cell with non-toxic buffer layer: A study on the sulphurization temperature and absorber layer thickness, 207, 419-427, 2020. https://doi.org/10.1016/j.solener.2020.06.103

[56] M.Y. Valakh, O. Kolomys, S. Ponomaryov, V. Yukhymchuk, I. Babichuk, V. Izquierdo-Roca, E. Saucedo, A. Perez-Rodriguez, J.R. Morante, S. Schorr and I. V. Bodnar, Raman scattering and disorder effect in Cu2ZnSnS4, 7, 258-261, 2013. https://doi.org/10.1002/pssr.201307073

[57] X. Liu, X. Li, X. Li, Q. Li, D. Zhang, N. Yu and S. Wang, Fabrication of Cu2SnS3 thin film solar cells via a sol-gel technique in air, Physica B: Condensed Matter, 627, 413613, 2022. https://doi.org/10.1016/j.physb.2021.413613

[58] M.A. Olgar, Improvement in the structural and optical properties of Cu2SnS3 (CTS) thin films through soft-annealing treatment, Superlattice Microst, 138, 106366, 2020. https://doi.org/10.1016/j.spmi.2019.106366

[59] J. Pankove, Photoelectric Emission, Optical Processes in Semiconductors, Dover Publications Inc., New York, 287, 301, 1971.

[60] J. Tauc, Optical properties and electronic structure of amorphous Ge and Si, Mater. Res. Bull., 3, 37-46, 1968. https://doi.org/10.1016/0025-5408(68)90023-8

[61] W. Wang, M.T. Winkler, O. Gunawan, T. Gokmen, T.K. Todorov, Y. Zhu and D.B. Mitzi, Device characteristics of CZTSSe thin-film solar cells with 12.6% efficiency, Advanced energy materials, 4, 1301465, 2014. https://doi.org/10.1002/aenm.201301465.

[62] C. Kim and S. Hong, Band gap shift of Cu2ZnSnS4 thin film by residual stress, Journal of Alloys and Compounds, 799, 247-255, 2019. https://doi.org/10.1016/j.jallcom.2019.05.290

[63] S. Chen, X.-G. Gong, A. Walsh and S.-H. Wei, Structural, electronic and defect properties of Cu2ZnSn (S, Se) 4 alloys, MRS Online Proceedings Library (OPL), 1370, 2011. https://doi.org/10.1557/opl.2011.764

[64] D. Han, Y. Sun, J. Bang, Y. Zhang, H.-B. Sun, X.-B. Li and S.J.P.R.B. Zhang, Deep electron traps and origin of p-type conductivity in the earth-abundant solar-cell material Cu2ZnSnS4, 87, 155206, 2013. https://doi.org/10.1103/PhysRevB.87.155206.